Supplementary Information for

A Novel and Accurate Microfluidic Assay of CD62L in Bladder Cancer Serum Samples

Gayatri S. Phadke,[a†] Jennifer E. Satterwhite-Warden,[a†] Dharamainder Choudhary,[b] John A. Taylor III,[c] and James F. Rusling[abde]

[a.] *Department of Chemistry (U-3060), University of Connecticut, 55 North Eagleville Road, Storrs, Connecticut 06269, United States.*
[b.] *Department of Surgery, University of Connecticut Health Center, Farmington, Connecticut 06032, United States.*
[c.] *Department of Urology, University of Kansas Medical Center, Kansas City, Kansas 66160, United States.*
[d.] *Institute of Materials Science, University of Connecticut, 97 North Eagleville Road, Storrs, Connecticut 06269, United States.*
[e.] *School of Chemistry, National University of Ireland, Galway, University Road, Galway, Ireland.*
† Both authors contributed equally to this paper.
* Correspondence should be addressed to J.F.R. (james.rusling@uconn.edu).

S-1: Extended experimental procedures

Materials and equipment

Screen-printed 8-electrode carbon array (700 μm diameter) sensors were purchased from Kanichi Research Services Ltd (Manchester, England). L-glutathione reduced (GSH, ≥98%), gold (III) chloride trihydrate ($HAuCl_4 \cdot 3H_2O$, ≥99.9%), sodium borohydride ($NaBH_4$, 99%), poly(diallydimethylammonium chloride) (PDDA, MW 200,000-300,000, 20% in water), 1-(3-(dimethylamino)propyl)-3-ethylcarbodiimide hydrochloride (EDC), N-hydroxysulfosuccinimide (NHSS), bovine serum albumin (BSA), calf serum, Tween-20, sodium chloride (NaCl), potassium chloride (KCl), sodium phosphate dibasic (Na_2HPO_4, ≥98%), sodium phosphate monobasic monohydrate ($NaH_2PO_4 \cdot 3H_2O$, ≥98%), hydroquinone (HQ, ≥99%), hydrogen peroxide (H_2O_2, 30%) were purchased from Sigma-Aldrich (St. Louis, MO, USA). The polydimethylsiloxane (PDMS) kit was obtained from Dow Corning (Auburn, MI, USA). Streptavidin-coated superparamagnetic beads (MP, 1 μm Dynabeads) and biotinylated horseradish peroxidase (HRP, 2.5 mg mL^{-1}) were purchased from Life Technologies (Carlsbad, CA, USA). All solutions were prepared using 18 MΩ-cm water purified by passing house-distilled water through a Hydro Service and Supplies purification system (Durham, NC, USA).

Monoclonal anti-human L-Selectin (CD62L) antibody (Ab_1, Catalog Number: BBA24, Clone: 4G8), biotinylated anti-human L-Selectin antibody (Ab_2, Catalog Number: BAF728), recombinant human L-Selectin/CD62L protein antigen (Ag, Catalog Number: ADP2), and Human sL-Selectin/CD62L ELISA kit (Catalog Number: BBE4B) were purchased from R&D Systems (Minneapolis, MN, USA). Human serum samples were collected from patients at the University of Connecticut Health Center (UCHC). Upon approval from the IRB and Written Informed Consent from patients sample collection was completed. All samples were stored at or below -80°C until used. Absorbances were measured for each assay experiment using FlexStation 3 multi-mode microplate reader (Molecular Devices, Sunnyvale, CA, USA). CHI 1040C multipotentiostat (Texas) was used for 8-channel amperometric detection.

Fabrication of immunoarray sensor

Screen-printed 8-electrode carbon array sensors were fabricated as previously described.[1-4] Briefly, arrays were coated with successive layers of polycation PDDA and negatively charged 5 nm glutathione-coated gold nanoparticles (GSH-AuNPs) using layer-by-layer (LBL) electrostatic adsorption for 20 min each as previously reported and as illustrated in Fig. S1A.[4,5] Incubating a freshly prepared crosslinking solution of EDC and NHSS for 10 min activated terminal surface carboxyl groups on the GSH-AuNP layer. The electrode sensor arrays were subsequently spotted with primary antibody (Ab_1), which was allowed to incubate overnight at 4°C resulting in Ab_1 immobilization via an amidation reaction, Fig. S1A.[3,4] Furthermore, prior to utilizing, the arrays were blocked with 2% BSA in PBS for 1 hr at 4°C to inhibit non-specific binding (NSB).

Preparation of bioconjugates

A previous protocol was implemented for the attachment of numerous biotinylated-Ab_2 and biotinylated-HRP labels to 1 μm diameter streptavidin-coated superparamagnetic beads (MPs, 10 mg mL^{-1}), as illustrated in Fig. S1A.[1-234,6] Briefly, MPs were magnetically separated using an Invitrogen DynaMag spin magnet and subsequently washed with PBS pH 7.4 three separate times. Then simultaneously biotinylated-Ab_2 and biotinylated-HRP were added into the MP dispersion containing 0.1% BSA in PBS pH 7.4 at a ratio of 1:2:4:4 (MP:Ab_2:HRP:BSA) followed by incubation at 37°C for 30 min. After conjugation, the bead bioconjugate (MP-Ab_2-HRP, Fig. S1A) dispersion was magnetically separated and washed three distinct times with 0.1% BSA in PBS pH 7.4 to remove any NSB Ab_2 and HRP. Lastly, the bioconjugate was then reconstituted with 0.1% BSA in PBS pH 7.4 and stored at 4°C until needed. Once optimized concentrations of both Ab_2 and HRP were determined, characterization assays were completed. Specifically, the average number of Ab_2 per MP was 2,100 (± 200), estimated via bicinchoninic acid assay (BCA) kit (Thermo Scientific, Rockland, IL, USA).[7] In addition, the average number of HRP per MP was estimated to be 5,000 (± 400) by 2,2'-azino-bis(3 ethylbenzthiazoine-6-sulfonic acid) (ABTS) end-point assay (Sigma Aldrich, St. Louis, MO, USA).[8,9] Absorbances were measured for each assay experiment using FlexStation 3 multi-mode microplate reader (Molecular Devices, Sunnyvale, CA, USA).

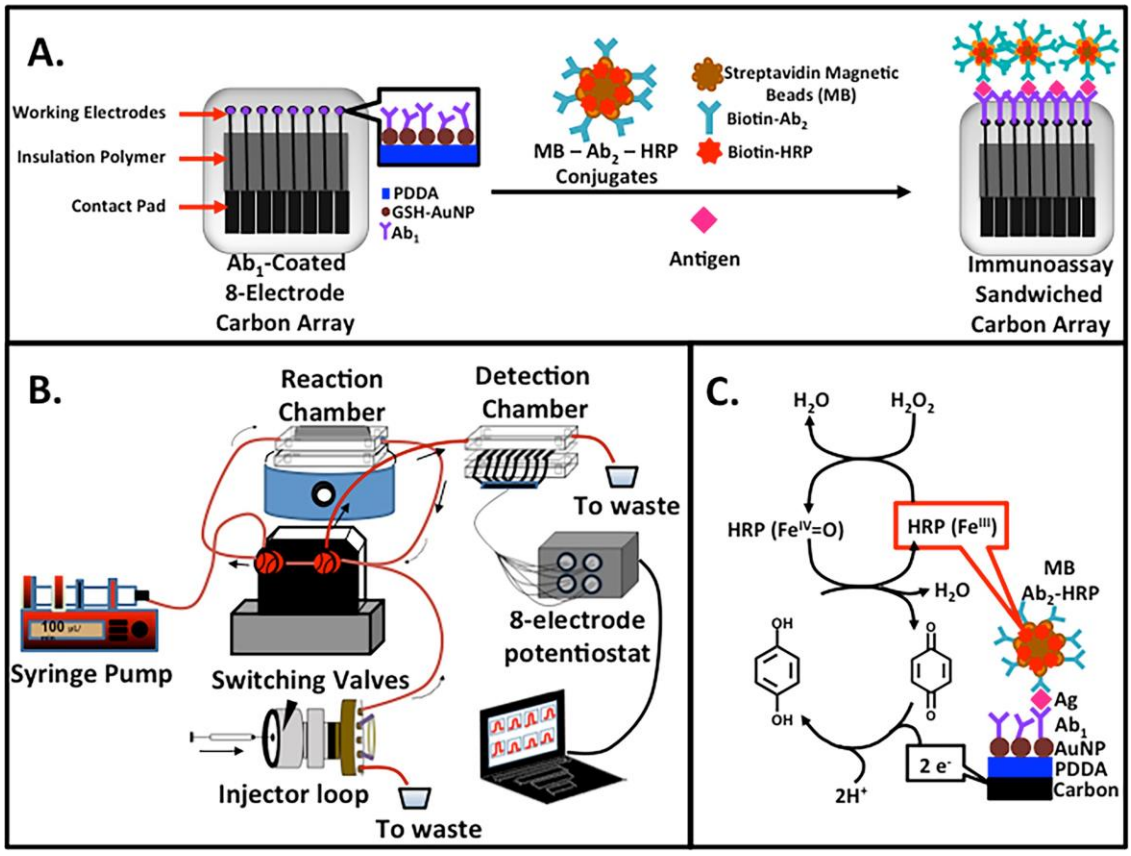

Fig. S1 Schematic illustration of the online-capture microfluidic assay. A) Strategy for modified ELISA was performed on B) a modular semi-automatic setup, where MB-Ab_2-HRP conjugate was incubated with antigen in an online capture chamber and then flowed to the detection chamber for incubation with surface-bound primary antibodies. C) 1 mM HQ and 0.1 mM H_2O_2 was injected for quantitative amperometric detection.

On-line capture and detection protocol

The general immunoassay capture strategy is illustrated in Fig. S1. An established modular on-line protein capture microfluidic system was employed, as shown in Fig. S1B, and this system provided a semi-automated methodology for protein detection. Construction details hve been reported previously.[1,2] More specifically, the system was constructed with an on-line capture chamber upstream from a detection chamber encasing an 8-electrode modified sensor array. Molded PDMS encased in hard plastic was used to create microfludiic channels in the capture and detection chambers. This modular microfluidic system was previously reported; however, further detail on assay performance will be briefly described.[1,2,10]

To begin, the system was first subjected to a flow of water followed by PBS-Tween 20. The detergent solution was used to minimize adhesion and NSB of undesirable molecules. Once the fluidic system was washed, 50 µL of bioconjugate (MP-Ab_2-HRP) was added to 150 µL of 20 mM PBS pH 7.4. This bioconjugate dispersion was then loaded into a 100 µL sample loop, injected at 100 µL min^{-1}, and allowed to fill the capture chamber. Next, protein antigen (standard or patient sample) in diluted calf serum was loaded and then injected into the capture chamber. Once the capture chamber was filled, stirring within the chamber was allowed for 30 min to facilitate protein capture. Throughout both sequentially injections, a magnet bar was held atop the capture chamber to ensure MP-Ab_2-HRP were captured.

After the 30 min incubation period, resultant protein antigen-MP-Ab_2-HRP bioconjugates were transferred to the detection chamber, which was housing a CD62L Ab_1 modified 8-electrode immunoarray, by switching the valves in the proper direction and pumping PBS-Tween 20 at 100 µL min^{-1} carried the protein antigen-MP-Ab_2-HRP into the detection chamber. The flow was stopped once the red-brown color of MPs filled the entire channel; this provided an indication the transfer process was complete. Bioconjugates incubated at the

electrode surfaces for 15 min to allow efficient capturing and completion of the immunoarray sandwich, Fig. S1A. PBS-Tween 20 flow resumed to remove any unbound bioconjugates followed by further washing with hydroquinone (HQ) for production of an electrochemical background signal. Amperometric detection was completed at -0.2 V vs. Ag/AgCl by injecting a mixture of 1 mM HQ mediator and 0.1 mM hydrogen peroxide (H_2O_2) in PBS at 100 µL min^{-1} into the detection chamber via the sample loop to activate the HRP labels on the bioconjugates. Prior to detection, the 8-electrode sensor array, platinum (Pt) counter, and Ag/AgCl reference were connected to a CHI 1040BC multipotentiostat (Fig. S1B). An electrochemical redox-cycle, Fig. S1C, transpired and current signals developed.[1,2,5, 11] Amperometric current signals are proportional to concentration of protein analyte. Once electrochemical detection was complete, a fresh modified 8-electrode array was inserted into the detection chamber for exposure to the next sample, which was still undergoing protein capture.

S-2: Optimization of HRP and antibodies

Optimization of enzyme label

Enzyme labels densely attached onto MP bioconjugates were optimized prior to finalizing CD62L protein antibody concentrations. This critical optimization step permits extension of the dynamic range from pg mL^{-1} to ng mL^{-1}. In particular, four different sets of MPs with varying concentrations of biotin-HRP labels, specifically 0.25, 0.5, 1.25 and 2.5 mg mL^{-1}, and a constant concentration of Ab_2 were prepared as descirbed in S-1. Following preparation, assays were performed by injection of a control (0 ng mL^{-1}), low (1 ng mL^{-1}), and high (10 ng mL^{-1}) antigen sample for each respective biotin–HRP concentration. Since the observed LOD prior to optimization was well below our requirements, HRP concentration was chosen to maximize the sensitivity (i.e., signal difference) between two tested CD62L concentrations in the ng ml^{-1} range. As observed in Fig. S2A, 0.5 mg mL^{-1} biotin–HRP provided the greatest signal difference between low (1 ng mL^{-1}) and high (10 ng mL^{-1}) CD62L concentrations and therefore, could possibly yield the highest sensitivity for the ng mL^{-1} dynamic range. Thus, 0.5 mg mL^{-1} was utilized for further optimization processes and attainment of the standard calibration curve.

Optimization of antibodies for protein CD62L

In addition to enzyme label, the capture antibody (Ab_1) and detection antibody (Ab_2) bound on the immunoarray platform and MP bioconjugate respectively were critically optimized to achieve maximum signal sensitivity prior to execution of a standard calibration curve. First, the detection antibody was optimized. In particular, the concentration of HRP and Ab_1 were kept constant and MP bioconjugates were prepared with three different Ab_2 concentrations, specifically 5, 10 and 20 µg mL^{-1}. Subsequently, assays were performed by injection of a control (0 ng mL^{-1}), low (1 ng mL^{-1}), and high (10 ng mL^{-1}) antigen sample for

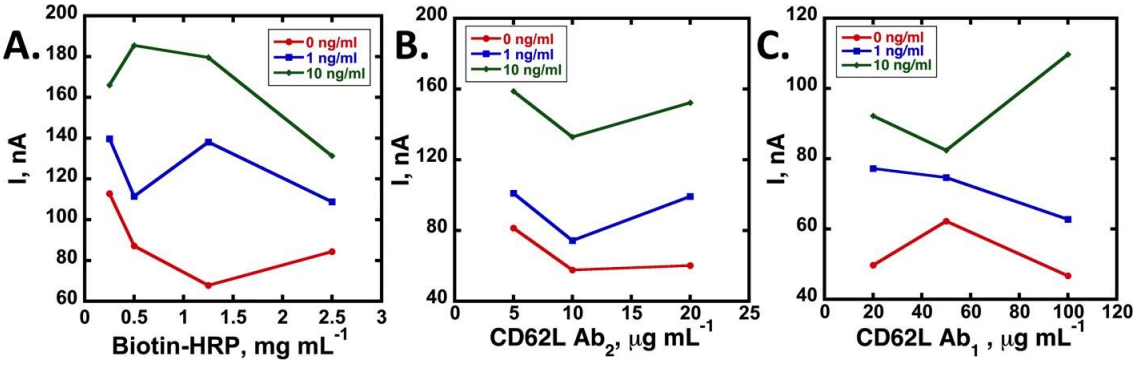

Fig. S2 Optimization results for CD62L sandwich immunoarray performance upon employing standard concentrations of 0, 1 and 10 ng mL^{-1}. A) Optimization of Biotin-HRP using consistent Ab_1 and Ab_2 concentrations. Optimal concentration of biotin-HRP was determined to be 0.5 mg mL^{-1}. B) Optimized result for secondary antibody (Ab_2) using consistent Ab_1 and biotin-HRP label concentrations. Optimal concentration of Ab_2 was determined to be 10 µg mL^{-1} and C) Optimized outcome for primary antibody (Ab_1) using consistent Ab_2 and biotin-HRP label concentrations. Optimal concentration of Ab_1 was determined to be 100 µg mL^{-1}.

each respective bioconjugate concentration and amperometric current signals were compared. The optimum concentration of 10 μg mL^{-1} Ab_2 was selected, as shown in Fig. S2B.

The concentration of the primary antibody is crucial as this improves assay sensitivity and minimizes NSB. Therefore, arrays with varying concentrations of Ab_1, specifically 5, 20, and 100 μg mL^{-1}, were prepared and the immunoassay was completed by the aforementioned procedure. During this Ab_1 optimization process, Ab_2 and biotin–HRP concentrations were kept constant. After comparison between each of the amperometric current signals, 100 μg mL^{-1} Ab_1 was selected and employed as the optimum concentration, as indicated in Fig. S2C.

Therefore, the best immunoarray performance was obtained when 100 μg mL^{-1} Ab_1 was bound on the sensor surface, while 10 μg mL^{-1} Ab_2 and 0.5 mg mL^{-1} biotin–HRP were attached to the MP bioconjugates. These conditions were employed for all latter experiments.

S-3: Stability of calibration signal

To assess stability of calibration signal after optimization of enzyme labels and antibodies, three selected concentrations, a control (0 ng mL^{-1}), low (1 ng mL^{-1}), and high (10 ng mL^{-1}) antigen samples were run on immunoarray system on different days to test reproducibility of the amperometric signal. Signals demonstrated good reproducibility as observed by relative standard deviations of less than 5%, at days 1, 145, 300, and 470 (as seen in Fig. S3A).

Additionally, the stability of the Ab_1 modified kanichi arrays was scrutinized up to 7 days after modification. The Ab_1-modified kanichi arrays were stored at 4°C in a moist chamber. To test stability, a control (0 ng mL^{-1}), low (1 ng mL^{-1}), and high (10 ng mL^{-1}) antigen samples were run on the immunoarray method. Minimal change in the amperometric response was observed, as seen in Fig. S3B, indicating the Ab_1-modified arrays to be stable for up to 1 week.

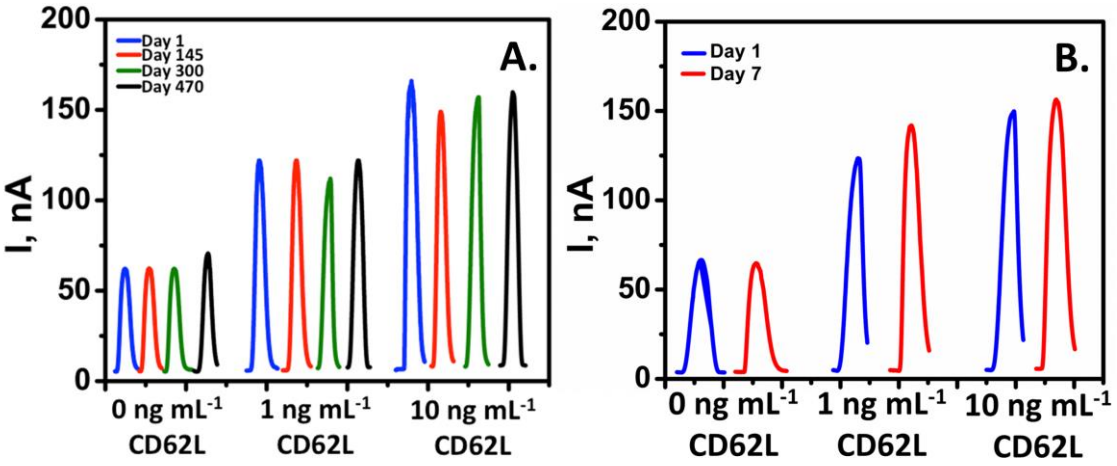

Fig. S3 Amperometric signals to demonstrate assay reliability and stability. A) Current signals from four independent days for 0, 1, and 10 ng mL^{-1} CD62L. B) Comparison of current signals indicating stability of surface bound Ab_1 on the LBL sensor array over duration of one week for 0, 1, and 10 ng mL^{-1} CD62L.

S-4: T-test analysis for spiked sample recoveries

To identify a potential systematic error with the CD62L ELISA assay, a one sample mean t-test was performed for individual spiking levels, for each detection method.[12] More specifically, lower and upper concentration limits at 95% CI were calculated for individual recovery levels, as shown in Table S1. The detection method under consideration was accurate if the corresponding true spiked level was within the calculated range (For

example, 75 ng mL^{-1} lies within the limits of 53.26 – 97.44). This test was also performed at 90% CI and yielded similar results (data not shown).
From Table S1, we concluded that significant bias exists outside the concentration range of 350 – 1500 ng mL^{-1} for ELISA. Such trend was not observed for our method; specifically the immunoarray detection method yielded recovery concentrations statistically similar to true spiked levels at 95% CI at all spiked levels. Furthermore, the immunoarray and ELISA methods was compared by using the two sample mean t-test.[12] Specifically, in our case, null hypothesis was set such that the recovered ELISA concentrations would equal the recovered immunoarray concentrations. In this case, $t_{statistical} > t_{critical}$ ($P < 0.05$) signified statistically relevant difference in recoveries. Upon comparison at each spiked level per methodology, we concluded that good correlation existed for the CD62L range of 350 – 1500 ng mL^{-1}, with exception of 550 ng mL^{-1} (Table S1). These results indicate better accuracy of the microfluidic CD62L immunoassay over the ELISA method, and reveal large systematic errors at the low and high concentration ranges for the ELISA kit.

Table S1 Sample mean t-tests for spiked sample recoveries

Spiked Level (ng mL^{-1})	Immunoarray Calculated conc. Range	Immunoarray T-test at 95% CI	ELISA Calculated conc. Range	ELISA T-test at 95% CI	Two sample mean t-test at 95% CI*
75	53.26 – 97.44	no diff.	18.95 – 35.97	sig. diff.	sig. diff.
250	201.1 – 304.8	no diff.	169.7 – 221.9	sig. diff.	sig. diff.
350	249.0 – 425.4	no diff.	121.2 – 493.2	no diff.	no diff.
550	555.9 – 641.9	no diff.	290.4 – 623.4	no diff.	sig. diff.
700	565.0 – 739.4	no diff.	578.6 – 784.8	no diff.	no diff.
1500	1008 – 1844	no diff.	280.0 – 2333	no diff.	no diff.
3000	2722 – 3763	no diff.	601.7 – 2250	sig. diff.	sig. diff.
5500	4305 – 6681	no diff.	921.4 – 4465	sig. diff.	sig. diff.

***** represents two sample mean t-test analysis for the null hypothesis, ELISA recovered concentration = Immunoarray recovered concentration
sig. diff. represents significantly different based on $t_{statistical} > t_{critical}$ or $P < 0.05$
no diff. represents statistically similar based on $t_{statistical} < t_{critical}$ or $P > 0.05$

S-5: Correlation between immunoarray and ELISA spiked sample recoveries

Results in Fig. 2A and Table S1 that confirm the accuracy of the immunoarray. Correlation plots for spiked sample analyses, plotting ELISA recoveries versus true spiking levels (Fig. 2C), immunoarray recoveries against spiked levels (Fig. 2D), provide further information on the accuracy of ELISA method. A slope of 1.0 and y-intercept of 0 ± 3SD indicates that the two analytical methods correlate very well, i.e. recoveries from both methods would be statistically similar. Verification of statistically relevant differences in slopes was performed by linear regression t-tests at 95% confidence interval (CI).[13]
Recovered concentrations in comparison to true spiked levels were utilized, and resultant information from linear regression t-Test was evaluated upon differences observed in $t_{statistical}$ and $t_{critical}$. Specifically, $t_{statistical}$ was calculated using deviation from expected slope of 1 and observed standard error of the slope. Meanwhile, $t_{critical}$ was a tabulated value from required CI and degrees of freedom.[12] In cases where $t_{statistical} > t_{critical}$ ($P < 0.05$), deviations from expected results are statistically significant.
As observed in Table S2, the only concentration recoveries that were statistically similar to true spiked concentrations ($P > 0.05$) were for the immunoarray detection method. ELISA recoveries compared to true spiked levels were statistically different at $P = <0.00001$. Hence, these results strongly demonstrated the presence of systematic error in the ELISA method.

Table S2 Linear regression t-test for spiked sample correlation plots

Linear Regression Plot	Slope ± SD	y-intercept ± SD (ng mL^{-1})	T-Test at 95% CI
Immunoarray vs. Spiked level*	1.013 ± 0.020	0.1298 ± 46.86	no diff.
ELISA vs. Spiked level*	0.455 ± 0.038	195.1 ± 75.3	sig. diff.

* n = 8, Null hypothesis was slope of correlation plot = 1.
sig. diff. represents significantly different based on $t_{statistical} > t_{critical}$ or $P < 0.05$
no diff. represents statistically similar based on $t_{statistical} < t_{critical}$ or $P > 0.05$

S-6: Assessing specificity of immunoarray method in bladder cancer tumor staging

The box plots (Fig. 3) demonstrated similar trends between the bladder cancer tumor stages for both ELISA and immunoarray. Therefore, to confirm specificity of differentiation between patient sample subsets (cancer-free controls, low-grade, and high-grade tumors), Two Sample Mean T-Test was performed at 95% CI (Table S3). The null hypothesis was set such that the average recovered CD62L concentration for subset 1 was equal to subset 2. In this case, $t_{statistical} > t_{critical}$ ($P < 0.05$) signified statistically relevant difference between the recovered CD62L concentrations for the subsets under consideration, i.e. the method is able to distinguish between the two patient sample subsets.

Table S3 Two sample mean t-test to differentiate patient sample subsets.

Patient Sample Subset Comparison Type	Assay Type	Two Sample Mean T-Test at 95% CI*
Cancer-free controls vs. All cancers	Immunoarray	sig. diff.
	ELISA	sig. diff.
Cancer-free controls vs. Low-grade tumors	Immunoarray	sig. diff.
	ELISA	sig. diff.
Cancer-free controls vs. High-grade tumors	Immunoarray	sig. diff.
	ELISA	sig. diff.
Low-grade vs. High-grade tumors	Immunoarray	sig. diff.
	ELISA	sig. diff.

* n = 10 for cancer-free controls patient subset, n = 11 for low-grade tumors subset, and n = 10 for high-grade tumors.
Null hypothesis was set as, mean of patient sample subset 1 = mean of patient sample subset 2.
sig. diff. represents significantly different based on $t_{statistical} > t_{critical}$ or $P < 0.05$
no diff. represents statistically similar based on $t_{statistical} < t_{critical}$ or $P > 0.05$

From Table S3, both assay detection methods distinguished tumor grade based upon circulating detected CD62L. Although both assay detection methods differentiate between patient sample subsets, the immunoarray method performs at a higher confidence level ($P_{Immunoarray} << P_{ELISA}$).

S-7: ROC characteristics for patient sample analysis by immunoarray method

ROC plots are generated by plotting true positive rate (sensitivity) vs. false positive rate (specificity) for a series of threshold concentration levels.[13] ROC plots are utilizied to distinguish cancer-free controls clinical samples versus cancer samples. In order to perfectly differentiate patients with and without cancer, an ROC plot must demonstrate 100% sensitivity, 100% specificity, and area under the curve (AUC) of 1.0.

Table S4 ROC analysis parameters for patient sample subsets.

ROC Comparison	Assay Type	Sensitivity	Specificity	AUC	Criterion
Cancer-free controls vs. All cancers	Immunoarray	100.00	100.00	1.000	>649.7
	ELISA	90.48	80.00	0.787	>873.8
Cancer-free controls vs. Low-grade tumors	Immunoarray	100.00	100.00	1.000	>649.7
	ELISA	81.82	80.00	0.836	>873.8
Cancer-free controls vs. High-grade tumors	Immunoarray	100.00	100.00	1.000	>649.7
	ELISA	90.00	100.00	0.980	>1291
Low-grade vs. High-grade tumors	Immunoarray	90.00	90.91	0.918	>3010
	ELISA	90.00	90.91	0.909	>1401

S-8: Assay validation for patient sample analysis with t-tests

Patient sample recoveries for all 31 samples (cancer-free controls and cancer) from the immunoarray method when plotted against ELISA recoveries (for the same samples) has a linear correlation with R^2 = 0.774. However the slope (3.00 ± 0.33) deviated from the "full correlation" value of 1 and the y-intercept differed from "full correlation" value of zero (-1464 ± 458) (Fig. 5). These results were significantly different from expected linear correlation (slope = 1 and y-intercept = 0), when subjected to linear regression t-test (performed as explained in S-5) at 95% CI ($P < 0.05$) (Table S5) and at 90% CI (data not shown).

Due to the observed deviations between standard CD62L ELISA and the immunoarray method, systematic error in ELISA for patient sample analysis was also suspected. Therefore, to investigate this possibility, linear regression t-test was done between correlation plots for patient sample recoveries (Fig. 5) and spiked sample recoveries (Fig. S4).This t-test yielded P = 0.1079 at 95% CI and since $P > 0.05$, systematic error in CD62L ELISA was uniformly present in both spiked and patient sample analysis, as noted in Table S5. Moreover,

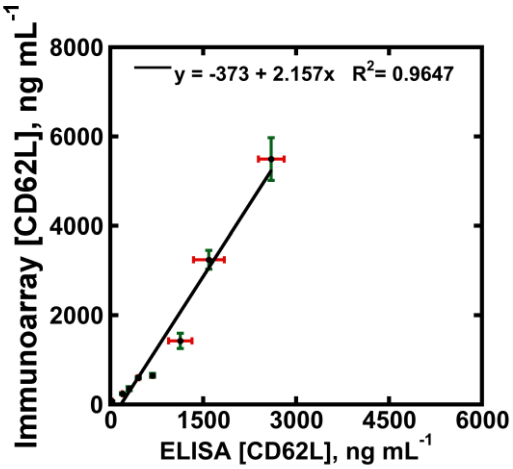

Fig. S4 Linear correlation plot for immunoarray vs. ELISA results for detection of CD62L in spiked samples. ELISA underestimates spiked sample CD62L levels, as seen by slope = 2.16.

Table S5 Linear regression t-test for patient sample correlation plot

Sample Type	Average Concentration ± SD (ng mL^{-1})		Paired T-Test at 95% CI*
	Immunoarray	ELISA	
Cancer-free controls	367.4 ± 141.8	811.3 ± 237.1	sig. diff.
Low-grade tumors	2243 ± 839	1151 ± 250	sig. diff.
High-grade tumors	4551 ±1662	1895 ± 539	sig. diff.

§ n = 8 for spiked sample correlation plot

‡ n = 31 for patient sample correlation plot

Null hypothesis was slope of correlation plot = 1.

***** represents statistically similar systematic error between the patient sample recoveries and spiked sample recoveries, as analyzed by linear regression t-test

sig. diff. represents significantly different based on $t_{statistical} > t_{critical}$ or $P < 0.05$

no diff. represents statistically similar based on $t_{statistical} < t_{critical}$ or $P > 0.05$

similar to patient sample correlation, spiked samples correlation plot different significantly from expected linear plot with slope =1 and y-intercept = 0.

Furthermore, patient sample subset means for both detection methods were analyzed by implementing a Paired T-Test.[12] Mean differences and standard deviation between the paired samples recoveries provided a $t_{statistical}$ value; meanwhile, $t_{critical}$ was calculated as mentioned previously. In cases where $t_{statistical} > t_{critical}$ ($P < 0.05$) deviations from expected results are statistically significant. Calculations were performed at 95% CI (Table S6) and 90% CI (data not shown). This statistical result further validated the presence of systematic error in low and high concentration ranges for ELISA; therefore, the CD62L immunoarray still exhibited higher reliability.

Table S6 Paired t-test for comparison of accuracy in immunoarray and ELISA

Linear Regression Plot	Slope ± SD	y-intercept ± SD (ng mL^{-1})	T-Test at 95% CI
Spiked sample recoveries§ Immunoarray vs. ELISA	2.16 ± 0.17	-373 ± 201	sig. diff.*
Patient sample recoveries‡ Immunoarray vs. ELISA	3.00 ± 0.33	-1464 ± 458	sig. diff.*

***** n = 10 for cancer-free controls patient subset, n = 11 for low-grade tumors subset, and n = 10 for high-grade tumor subset.

Null hypothesis: Immunoarray detected concentration – ELISA detection concentration = 0.

sig. diff. represents significantly different based on $t_{statistical} > t_{critical}$ or $P < 0.05$

no diff. represents statistically similar based on $t_{statistical} < t_{critical}$ or $P > 0.05$

In conclusion, the patient sample recoveries with the bead-based immunoarray method provided more accurate estimates of circulating CD62L levels in patient serum than the ELISA assay kit. Further, the ELISA method underestimates CD62L concentration outside the range of 350 - 1500 ng mL^{-1}.

References

1 B. A. Otieno, C. E. Krause, A. Latus, B. V. Chikkaveeraiah, R. C. Faria and J. F. Rusling, *Biosens. Bioelectron.*, 2013, **53**, 268–274.

2 C. E. Krause, B. A. Otieno, G. W. Bishop, G. Phadke, L. Choquette, R. V. Lalla, D. E. Peterson and J. F. Rusling, *Anal. Bioanal. Chem.*, 2015, **407**, 7239–7243.

3 B. V. Chikkaveeraiah, V. Mani, V. Patel, J. S. Gutkind and J. F. Rusling, *Biosens. Bioelectron.*, 2011, **26**, 4477–4483.

4 R. Malhotra, V. Patel, B. V. Chikkaveeraiah, B. S. Munge, S. C. Cheong, R. B. Zain, M. T. Abraham, D. K. Dey, J. S. Gutkind and J. F. Rusling, *Anal. Chem.*, 2012, **84**, 6249–6255.

5 V. Mani, B. V. Chikkaveeraiah, V. Patel, J. S. Gutkind and J. F. Rusling, *ACS Nano*, 2009, **3**, 585–594.

6 B. A. Otieno, C. E. Krause and J. F. Rusling, *Meth. Enzymol.*, 2016, **571**, 135–150.

7 P. K. Smith, R. I. Krohn, G. T. Hermanson, A. K. Mallia, F. H. Gartner, M. D. Provenzano, E. K. Fujimoto, N. M. Goeke, B. J. Olson and D. C. Klenk, *Anal. Biochem.*, 1985, **150**, 76–85.

8 J. Keesey, *Biochemical Information*, 1st ed., Boehringer Mannheim Biochemicals, Indianapolis, 1987, pp. 58.

9 J. Pütter, R. Becker, In: *Methods of Enzymatic Analysis*; Bergmeyer, H.U, Ed., Verlag Chemie Weinheim, New York, 1983, **3**, p. 286–293.

10 C. K. Dixit, K. Kadimisetty, B. A. Otieno, C. Tang, S. Malla, C. E. Krause and J. F. Rusling, *Analyst*, 2016, **141**, 536–547.

11 C. E. Krause, B. A. Otieno, A. Latus, R. C. Faria, V. Patel, J. S. Gutkind and J. F. Rusling, *ChemistryOpen*, 2013, **2**, 141–145.

12 D. C. Harris, *Quantitative Chemical Analysis*, 7th ed, W.H. Freeman and Company, New York, 2007, p 57–62.

13 J. H. McDonald, *Handbook of Biological Statistics*, 3rd ed, Sparky House Publishing, Baltimore, 2014.